JOURNAL OF GEOPHYSICAL RESEARCH, VOL. 115, A02206, doi:10.1029/2009JA014456, 2010

Ten years of Hubble Space Telescope observations of the variation of the Jovian satellites' auroral footprint brightness

S. Wannawichian,[1] J. T. Clarke,[1] and J. D. Nichols[2]

Received 12 May 2009; revised 2 October 2009; accepted 6 October 2009; published 10 February 2010.

[1] During the past decade, FUV imaging of Jupiter's auroral region by the Hubble Space Telescope (HST) using two instruments, the Space Telescope Imaging Spectrograph (STIS) and the Advanced Camera for Surveys (ACS), has provided detailed information on the electrodynamic interaction between Io's, Ganymede's, and Europa's atmospheres and plasma in Jupiter's magnetosphere. This interaction is responsible for the satellites' auroral footprints in Jupiter's atmosphere connected via magnetic flux tubes to the satellites' interaction regions. The observed brightness of each auroral footprint is considered to be one main observable quantity to characterize the interaction environment at the satellites. Previous observations of Io's magnetic footprints using HST STIS images showed that the footprint emission appears brightest when Io is centered in the plasma torus. With the much larger data set obtained from the 2007 HST campaigns, we find the same variation observed by Serio and Clarke (2008), but with significantly better statistics over a time period of 10 years. These results confirm that Io's footprint brightness varies mainly with the satellite's location in Jupiter's plasma torus over a long time scale. Additional observations of the downstream emissions and their variations were presented by Bonfond et al. (2007). In Ganymede's case, the relation between the footprint brightness and the satellite's position in Jupiter's magnetosphere shows some evidence for the same general trend, although the data are noisier than the data for Io. Ganymede's footprint brightness appears to be less consistent over time than Io's. The variation of Ganymede's footprints over short time periods was studied by Grodent et al. (2009). Europa's fainter footprint brightness makes it difficult to see any systematic trend.

Citation: Wannawichian, S., J. T. Clarke, and J. D. Nichols (2010), Ten years of Hubble Space Telescope observations of the variation of the Jovian satellites' auroral footprint brightness, *J. Geophys. Res.*, *115*, A02206, doi:10.1029/2009JA014456.

1. Introduction

[2] A number of direct observations and theoretical studies of planetary aurora have provided fruitful information about their magnetospheres [*McPherron*, 1995; *Carlson and Egeland*, 1995; *Cowley*, 1998; *Kivelson*, 2005; *Stallard et al.*, 2008]. Jupiter's bright and complex auroral region has traditionally been divided into three regions: the main auroral emission, polar emission, and footprint emission [*Clarke et al.*, 1998; *Grodent et al.*, 2003; *Hill*, 2004]. Observations of Jupiter's decametric radiation (DAM) first showed the evidence of Io's strong influence on the variation of the emission's intensity [*Bigg*, 1964]. The electron energy and electric potential profile along the magnetic field line were later acquired on the basis of Jupiter's radio emissions [*Hess et al.*, 2008]. The first infrared observation of Io's footprint emission was presented by *Connerney et al.* [1993]. The observation showed faint H_3^+ emissions at the foot of the Io flux tube, ~8° equatorward from the main oval. Over the last decade, the Hubble Space Telescope (HST) has made a large number of FUV observations of the auroral footprints [*Clarke et al.*, 1998; *Gérard et al.*, 2006; *Grodent et al.*, 2008a; *Wannawichian et al.*, 2008; *Serio and Clarke*, 2008, hereafter SC08]. These studies of auroral magnetic footprints provide a significant step to understanding the satellites' roles in influencing planetary magnetospheres [*Kivelson et al.*, 2004; *Saur et al.*, 2004]. Io, for example, is known to be the main source of plasma in Jupiter's magnetosphere. Io's auroral footprint emission was found to be the brightest among the magnetic footprints of the Jovian satellites [*Clarke et al.*, 1998].

[3] Theoretical models describing the connections between Io and Jupiter's ionosphere include the unipolar magnetic field model [*Goldreich and Lynden-Bell*, 1969], the Alfvén wave model [*Goertz*, 1980; *Neubauer*, 1980; *Hill et al.*, 1983], and the open-loop Alfvén model [*Crary*, 1997; *Crary and Bagenal*, 1997]. According to the unipolar inductor model, a magnetic flux tube connects Io and Jupiter's iono-

[1]Center for Space Physics, Boston University, Boston, Massachusetts, USA.

[2]Department of Physics and Astronomy, University of Leicester, Leicester, UK.

0148-0227/10/2009JA014456$09.00

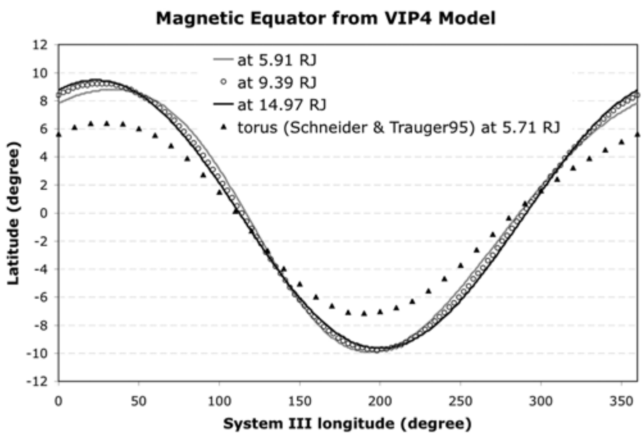

Figure 1. Locations of Jupiter's magnetic equator are calculated from the VIP4 magnetic field model [*Connerney et al.*, 1998] at distances 5.91 R_J, 9.39 R_J, and 14.97 R_J (R_J = 71,492 km) from Jupiter. These three distances correspond to orbital distances of Io, Europa, and Ganymede, respectively. The plot also includes the observed locations of the plasma torus' peak density [*Schneider and Trauger*, 1995] at 5.71 R_J.

sphere, creating a DC circuit in which a current is driven by a potential induced by the difference in velocity between Io, orbiting at the Keplerian velocity, and the surrounding corotating plasma. The current travels via Alfvén waves upward from Io into Jupiter's ionosphere and returns to Io to maintain a closed circuit. However, observations by Voyager 1 [*Broadfoot et al.*, 1979; *Bagenal and Sullivan*, 1981] made the first in situ measurement of Jupiter's plasma torus, which slows down the Alfvén waves. The Alfvénic travel time was found to be longer than the time predicted by the steady state unipolar inductor model [*Bagenal*, 1994], implying that the direct current loop cannot close between Io and Jupiter's ionosphere. The Alfvén wave model proposes a different explanation of the interaction between the corotating torus plasma and the plasma near Io [*Goertz*, 1980; *Neubauer*, 1980; *Hill et al.*, 1983]. In this model, the torus plasma, traveling faster than the plasma in the immediate vicinity of Io, is decelerated, causing a perturbation in the local magnetic field, which propagates via Alfvén waves downstream along the field line. The magnetic field lines are compressed and bended because of this perturbation, creating a wake region, known as an "Alfvén wing," ahead of the satellite in the corotation direction. Near Io, the interaction region is characterized by two subsections: (1) the inner atmosphere, where the collisions between torus plasma and Io's neutral atmosphere dominate, and (2) the extended atmosphere, where the charged particles, ionized by charge exchange and electron impact, are picked up [*Delamere et al.*, 2003]. Third, a combination of the above models, the open-loop Alfvén model, has been proposed [*Crary*, 1997; *Crary and Bagenal*, 1997]. From observations of the Jovian DAM arcs [*Gurnett and Goertz*, 1981], the spacing of these arcs suggests that the Alfvén wave is trapped between Jupiter's ionosphere and high-latitude plasma, because of a reflection of the Alfvén wave at the boundary of the torus. The interaction begins with the Alfvén perturbation near Io and then evolves downstream into the steady state current that extends to the torus boundary [*Crary and Bagenal*, 1997]. Observationally, Io's FUV auroral footprints appear brightest when the satellite is in the center of the plasma torus [*Gérard et al.*, 2006; SC08], where the mass pickup is expected to be highest. These observations thus support the importance of mass pickup near the satellite. Therefore, the electrodynamic interactions at the satellites are suggested to be one controlling factor of the magnetic footprints in the auroral region. The strength and nature of the interactions will affect the observed footprint features, e.g., brightness, shape, and location [*Jacobsen et al.*, 2007; SC08; *Bonfond et al.*, 2008].

[4] Since the satellite's footprint brightness is controlled by the interaction between the satellite's atmosphere and the surrounding magnetospheric plasma, knowledge of the magnetospheric plasma structure, especially the plasma torus, in the vicinity of the satellites is essential to interpret the auroral footprint emission. The density distributions of ions and neutral particles in Jupiter's plasma torus have been studied via ground-based imaging by *Schneider and Trauger* [1995], who identified three different regions in the plasma torus: (1) the cold torus at 4.5–5.3 R_J; (2) the ribbon, the most prominent feature in Jupiter's torus, at 5.5–5.9 R_J; and (3) the warm torus at 5.9–7.5 R_J. *Schneider and Trauger* [1995, Table 3] shows the central latitude of the ribbon, which is defined by the latitude of the maximum density and varies with system III longitude (λ_{III}). A plot of their result is shown in Figure 1. The brightness of the ribbon was found to be most prominent between 150° and 300° λ_{III}, near the 110° and 290° λ_{III} intersections of the plasma equator with Io's orbit (5.91 R_J). A study of the plasma torus properties from direct observations by the Ultraviolet Imaging Spectrograph Subsystem (UVIS) on Cassini [*Steffl et al.*, 2004] also showed an asymmetry in EUV brightness between the dusk and dawn ansae. The various ranges of temporal variations in the plasma torus brightness were presented. Their results suggest a different plasma environment to that observed during the Voyager era [*Steffl et al.*, 2008]. Furthermore, evidence of an additional source of plasma in the torus near Europa's orbit was presented by empirical modeling of Voyager 1 observations [*Bagenal*, 1994]. Direct observations of the ion composition by several spacecraft (i.e., Voyager 1 and 2, Galileo, and Ulysses) have provided fruitful data for modeling plasma properties from 5 R_J to 12 R_J [*Bagenal*, 1994; *Moncuquet et al.*, 2002]. Although the plasma densities near Io measured by different spacecraft differ by less than one order of magnitude, in general, the density is suggested to be most concentrated near Io's orbit. Supporting those direct observations, UV imaging by HST (SC08) has revealed a strong relation between Io's magnetic footprint brightness and its location in Jupiter's plasma torus. In particular, the footprint is brightest when Io is at $\lambda_{III} \sim 110°$. Here we examine a significantly expanded data set and confirm the trend identified by SC08, but with considerably improved statistics. We also present additional results for Ganymede and Europa.

[5] For a detailed comparison of the observed footprint brightness with the plasma environment at the satellite, the locations of the plasma equator as a function of λ_{III} were studied. The plasma equator is the position of peak density in the plasma torus located between the magnetic equator and the centrifugal equator [*Schneider and Trauger*, 1995]. These results will demonstrate the significance and nature of

mass pickup processes near Io and also extend the analysis to the outer Jovian satellites, where different current sheet parameters, magnetospheric structure, and external influences, such as solar wind pressure, are expected.

2. Observations and Data Reduction

[6] HST has played a major role in imaging Jupiter's FUV (115–170 nm) aurora for more than 10 years. Two different instruments, the Space Telescope Imaging Spectrograph (STIS) and the Advanced Camera for Surveys (ACS), were used from 1997 to 2004 and 2005 to the present, respectively. The chosen HST data set for the present work comprises 242 images for Io, 14 images for Europa, and 48 images for Ganymede. The reduction procedures include dark image subtraction, flat-field correction, and instrumental geometric distortion correction [*Nichols et al.*, 2008; *Clarke et al.*, 2009]. The images were scaled to appear at the common distance of 4.2 AU, with the north pole oriented toward the top of the image and converted to kiloroentgens (1 kR = 10^9 photons cm^{-2} s^{-1} into 4π sr). The conversion factors were generated by the synthetic UV spectrum of H_2 and Ly α emission [*Gerard et al.*, 2002]. The signal-to-noise ratio was improved by two techniques: (1) accumulating a set of images taken in the same HST orbits and (2) subtracting the background consisting of the reflected sunlight attenuated by hydrocarbon hazes. In the case of the Ganymede footprint, which is close to the main oval, the background also includes the diffuse auroral emissions from the secondary oval and isolated features. The first technique was used with an exposure time of less than 100 s, in which three consecutive images were summed and averaged. For the second technique, the simulation of the background brightness is based on the reflected sunlight from Jupiter's atmosphere. The modified Minnaert formulation was used for the horizontal distribution [*Vincent et al.*, 2000], and a fit of the north–south banding pattern obtained from the sum of all the images obtained in a given month was used for the latitudinal variation [*Nichols et al.*, 2009; *Clarke et al.*, 1998; *Wannawichian et al.*, 2008]. Then the subtraction factor was chosen so that the resulting background level is no lower than 6 kR, referring to the emission of H Ly α from the planetary atmosphere. In addition to the global background produced by the Minnaert function, a linear interpolation of the local background brightness surrounding the footprint was produced because of the extension of the emission from the main oval. Then the simulated background was subtracted from the original image to acquire the footprint brightness. According to previous observations [*Clarke et al.*, 1998; *Gérard et al.*, 2006], Io's footprint could appear as multiple spots, presumably as a result of the Io-generated waves reflected at plasma density gradients in the plasma torus. In this paper, Io's footprint brightness is averaged over a 0.25 × 0.25 arc sec^2 area, which is smaller than areas used in previous studies [*Bonfond et al.*, 2007; SC08], to focus on the brightest spots.

3. Data Analysis

3.1. Magnetic Mapping and Footprint Prediction

[7] The VIP4 magnetic field model [*Connerney et al.*, 1998] was used to map the magnetic latitude and longitude of Io, Ganymede, and Europa onto Jupiter's ionosphere, given the satellites' system III longitude (λ_{III}) at each time. The VIP4 model as described by *Connerney et al.* [1998] predicts relatively well the location of Io's footprint, but it is more uncertain for Europa and Ganymede. Moreover, *Grodent et al.* [2008a] showed that the predicted locations of magnetic footprints for Io, Europa, and Ganymede are least accurate at the region called the "auroral kink sector." The kink sector is suggested to be controlled by a weakening of the surface magnetic field by a localized tilted dipole, the so-called "Dessler anomaly" [*Clarke et al.*, 2004]. In the case of Ganymede's footprints, in addition to the planetary magnetic field, the observed latitudes appear to be influenced by the external magnetic component produced by the azimuthal current flowing in the current sheet [*Grodent et al.*, 2008b]. In addition, since Ganymede's and Europa's footprints are predicted to be very close to the main oval, often the footprints blend into the main oval when they are near the limb or extended in latitude. Therefore, separating the footprints from the main oval can be challenging. This task includes carefully simulating the background, including the emission from the main oval to separate the footprint from the main oval emission.

3.2. Plasma Environment Near the Satellites

[8] The planetocentric latitude of the magnetic equator at the orbital distances of Io, Ganymede, and Europa versus λ_{III} was computed using the VIP4 magnetic field model (Figure 1). It is shown that the latitude of the magnetic equator is roughly independent of the distance from Jupiter. In Figure 1, the observed latitudes of the plasma equator at ~5.71 R_J [*Schneider and Trauger*, 1995] vary approximately sinusoidally with λ_{III}, roughly in phase with the variation of the latitude of the magnetic equator. According to *Khurana and Schwarzl* [2005], at distances less than 25 R_J from Jupiter, the current sheet appears to be more rigid than at greater distances, such that the distance of the current sheet from Jupiter's equatorial plane varies linearly with radial distance. Therefore, the latitude in degrees at the plasma equator at 5.71 R_J should plausibly be similar at distances within 25 R_J, covering the orbital distances of Io, Europa, and Ganymede. In addition, at λ_{III} ~ 110° and 290°, the magnetic equator and plasma equator cross 0° latitude, which corresponds to the satellites' orbital planes. Around those longitudes, a strong interaction is expected near the satellites because of the denser plasma environment. Consequently, the satellites' auroral footprint may be brighter.

3.3. Limb Brightening Effect

[9] Jupiter's atmosphere is mostly optically thin in H_2 emission but becomes optically thick in H Ly α emission. However, H Ly α emission is only 15% of the entire H_2 spectrum [*Grodent et al.*, 2003]. In an optically thin atmosphere, the footprint will appear brighter near the limb edge because of the longer line-of-sight column. However, the footprint also appears smaller, such that limb brightening does not affect the calculation of the total emitted power. Therefore, the observer's line of sight through this optically thin atmosphere, which relates to the distance to the limb, should not cause any variation in footprint brightness. The implication is that the variation in the

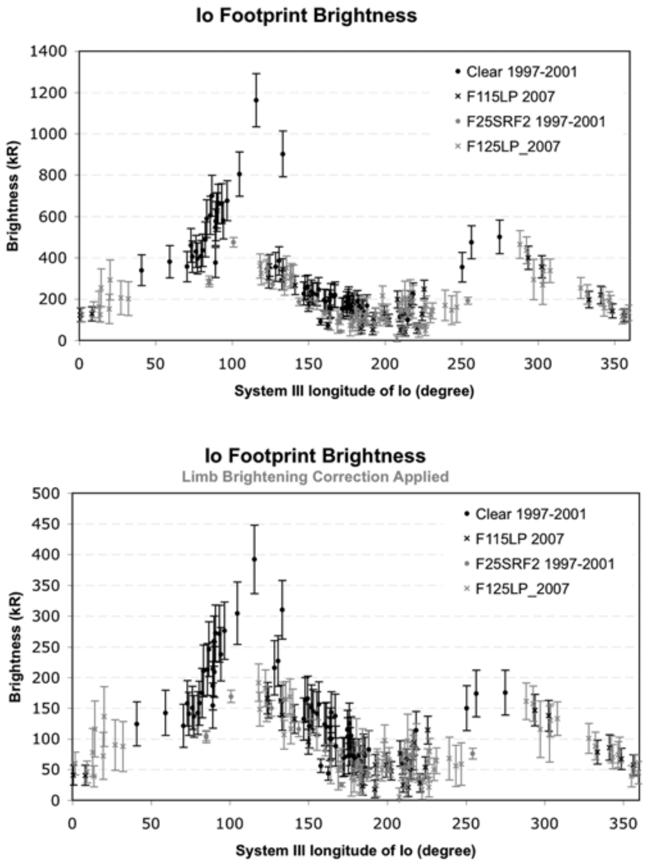

Figure 2. (top) Io's footprint brightness corresponding to the location of Io (λ_{III}). (bottom) Same as for Figure 2 (top) but with limb-brightening correction. The data are separated into two epochs, 1997–2001 and 2007, comparing clear (115–174 nm), F25SRF2 filter (130–174 nm), F115LP filter (115–170 nm), and F125LP filter (125–170 nm). The error bars are the Poisson uncertainty of the background's count rates of the regions near the footprints.

footprint's emitted power is independent of any application of limb brightening correction. However, there are some uncertainties, including the accumulation of extra emissions from the tail of the footprint (due to the wake in the interaction region at the satellites) and absorption in the optically thick hydrocarbon lower atmosphere. These uncertainties become significant when the footprint appears close to the limb.

[10] To test the effect of an optically thin atmosphere as well as other uncertainties, the calculation of the limb brightening correction factor at the emission scale height of 600 km was used according to the method described by SC08. Then the footprint brightness was divided by the correction factor to acquire the limb brightening corrected brightness. The correction factor varies as a function of distance from Jupiter's limb. We set the limit of the least distance to limb at 5000 km, where the limb brightening correction factor dramatically increases, causing a high uncertainty. We tested the effect of limb brightening by examining brightness profiles obtained with and without the limb brightening correction, and we show that within the uncertainties, the same general trends are seen in the data, as discussed in section 4.

4. Results: Footprints' Brightness and Locations of Io, Ganymede, and Europa

[11] The variation of the auroral footprint brightness as a function of Io's longitude (λ_{III}) is shown in Figure 2. The error bars are the Poisson uncertainty calculated from the background count rates in the region near the footprints. The effect of limb brightening is analyzed by comparing (Figure 2, top) Io's footprint brightness acquired directly from the images with (Figure 2, bottom) the same footprint brightness with the applied limb-brightening correction. The trend in the variation of footprint brightness is only slightly different when the limb brightening correction is applied. This was examined quantitatively by correlating the observed brightness values with the function $f = \sin^2(\lambda_{III} - \varphi)$, which reasonably well approximates the two-peaked structure of the data, and where phase φ was shifted in 1° steps from 0° to 360°. The locations of the fitted peaks are then given by $\varphi + 90$ and $\varphi + 270$. For each case, the phase with maximum correlation was determined, as was the longitude range inside in which the correlation coefficient was 90% of the maximum, as a reasonable estimation of the range of uncertainty. The locations of peaks thus determined are 107° and 287° ± 8° for the limb-brightening-corrected data and 101° and 281° ± 13° for the noncorrected data, i.e., essentially identical within the uncertainty. These results suggest that the relation between Io's location (λ_{III}) and the brightness of its magnetic footprint is not significantly affected by the uncertainty in the limb brightening. In addition, the variation as shown in Figure 2 (top) is in good agreement with previous observations by SC08. Observed over a longer time with more data points, our statistically improved data confirm the relation between Io's footprint brightness and Io's location. However, small variations of Io's footprint brightness were noticed, which requires a more detailed study and analysis. In addition, the second peak at $\lambda_{III} \sim 250°$–300° is seen more clearly compared with previous work (SC08). The peak brightness appears at two longitudes (λ_{III}), ~110° and ~290°, where Io is near the plasma equator. In Figure 2, footprints observed in clear images are generally brighter than those from filtered images. The analytical interpretation will be discussed in section 5.

[12] The situation is very different for Ganymede (Figure 3). The brightness variation of Ganymede's magnetic footprint appears more time variable. Compared to our results, observations were of different time variations of footprint brightness [*Grodent et al.*, 2009] for 100 s, 10–40 min, and 5 h time scales. Even though the relation between Ganymede's footprint brightness and the satellite's location is not as strong as it is in Io's case, there is a suggested peak feature at $\lambda_{III} \sim 100°$. As seen in Figure 4, we found fewer data for Europa's magnetic footprints. The data show a less clear relation between Europa's footprint brightness and the location of the satellite compared to those of Io and Ganymede. Even though the brightest footprints are observed when Europa was at $\lambda_{III} \sim 100°$, near the plasma equator, the faint emissions result in uncertainties

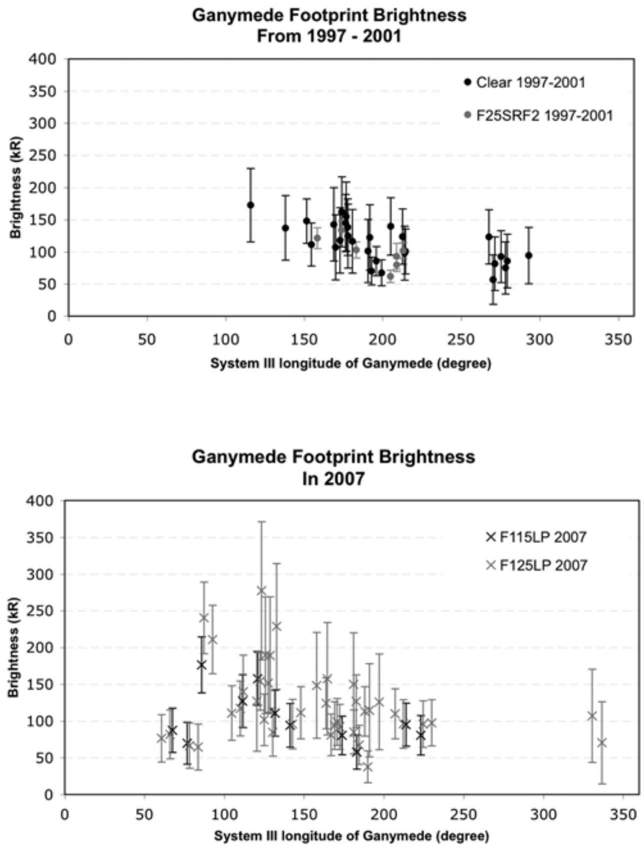

Figure 3. (top) Ganymede's footprint brightness corresponding to its λ_{III} location from 1997 to 2001. (bottom) Same for Figure 2 (top) but with images taken in 2007. The filters' notations are the same as described in Figure 2 (top) with no limb brightening correction.

too large to establish any trend. It is thus too early to conclude about the interaction at Europa.

5. Discussion

[13] These observations (Figure 2) confirm the same variation of Io's magnetic footprint brightness (brightest at $\lambda_{III} \sim$

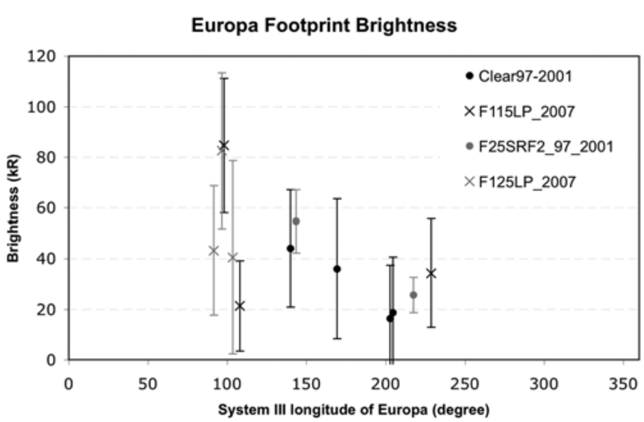

Figure 4. Europa's footprint brightness corresponding to its λ_{III} location from 1997 to 2007. The filters' notations are the same as described in Figure 2 (top) with no limb brightening correction.

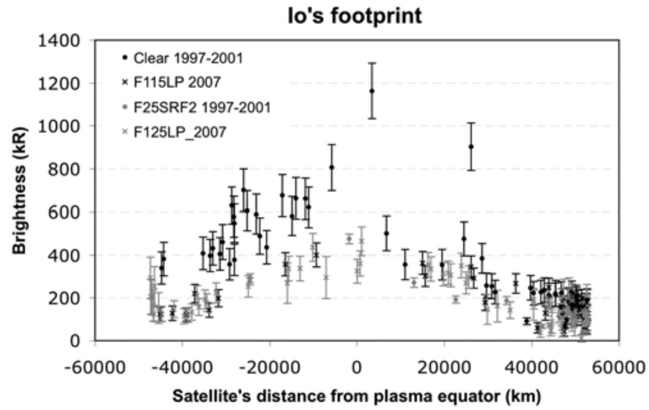

Figure 5. Io's footprint brightness from Figure 2 plotted as a function of the satellite's distance from the plasma equator. The distance is based on the latitudinal variation of the plasma equator at different λ_{III} (Figure 1). The negative distance is for the location where Io is below (south) the plasma equator.

110°) discussed earlier by SC08. One benefit of having longer observational time and better statistics is that we are able to see clearly the second peak at $\lambda_{III} \sim 270°$. According to ground-based observations [*Schneider and Trauger*, 1995], there is an "active sector" (the most observed intense emission) of the plasma torus between 150° and 300° λ_{III}. Schneider and Trauger also found the intersections of the plasma equator and Io's orbit at 110° and 290°. This information supports our observation of Io's footprint brightness maxima at ~110° and ~270° λ_{III}. Consistent results are also found from the observation of DAM bursts [*Bigg*, 1964], in which the highest intensities are found approximately within 115°–335° system III longitude of Jupiter, near an active sector, as discussed by *Schneider and Trauger* [1995]. In addition, the observation of H_3^+ emissions at the foot of the Io flux tube [*Connerney et al.*, 1993] presented Io's footprint locations, which appeared to be close to the locations predicted by the then-current model (GSFC O_6). Their results gave the first direct evidence of the coupling between Io and Jupiter's ionosphere.

[14] It is remarkable that the footprint brightness follows the same pattern despite the long period of observations (1997–2007). The pattern is relatively insensitive to temporal variations of the plasma environment and is determined mainly by Io's location in the torus. This result provides better statistical evidence that the interaction between Io's atmosphere and Jupiter's ionosphere is strongest when Io is in the center of the plasma torus. The comparison of Io's footprint brightness and the satellite's distance from the plasma equator [*Schneider and Trauger*, 1995] is presented in Figure 5. The results display a strong connection between the plasma environment near Io and its auroral footprint. The footprint brightness appears greater when the satellite is closer to the plasma equator.

[15] The brightness observed in the clear images (115–170 nm) is different from those observed in the filtered images (125–170 nm). In the reduction process, the different sensitivities between two band passes are compensated by the calibration procedure (converting count into kiloroentgens). These converting coefficients are calculated on the

Table 1. Correlation Coefficients Between Both Linear and Gaussian Functions of the Satellites' Distance From the Plasma Equator and Their Footprint Brightnesses[a]

	STIS		ACS		
Satellites	Clear	F25SRF2	F115LP	F125LP	Total
		Linear Correlation Coefficient			
Io	0.844	0.915	0.848	0.819	0.733
Ganymede	-	-	0.731	0.444	0.265
Europa	-	-	-	-	0.461
		Gaussian Correlation Coefficient			
Io	0.829	0.868	0.832	0.798	0.727
Ganymede	-	-	0.751	0.463	0.281
Europa	-	-	-	-	0.543

[a]Correlation coefficients are given in equation (1). The two variations result in similar correlation coefficients. The plasma density scale height, H, is 1 R_J, 1.49 R_J, and 1.32 R_J for Io, Europa, and Ganymede, respectively. The correlation coefficients among different filters are compared. Because of poor statistics, the correlation coefficient for Europa was calculated only for the entire data set.

basis of on the assumption that Jupiter's auroral spectrum is the same everywhere. However, the spectrum could vary at different times and locations. Therefore, the variation between clear and filtered images could be the result of variations in the auroral footprint's spectrum. In addition, regardless of how the limb brightening correction affects the overall footprint brightness, the trend in the variation is conserved (Figure 2). In the large scale, these results suggest the time independence of the footprint brightness. However, the more continuous and concentrated measurements for each day allow us to see small variations. It is possible that there are other controlling factors with larger amplitude for which more theoretical and analytical analysis are required. For example, Io's footprint brightness has been observed to brighten on the time scale of ~1 min [*Bonfond et al.*, 2007], suggested to be an effect of the acceleration mechanism of the electrons on their way to Jupiter.

[16] According to Table 1, the study of the correlation between Io's distance from the plasma equator and its footprint brightness shows very high linear correlations (more than 80%) for all the filters. However, *Hill and Michel* [1976] showed that the density of the plasma in the torus is expected to vary as a Gaussian from the magnetic equator. We have therefore also computed the correlation of the footprint brightness with the function

$$g = \exp\left(-d^2/H^2\right), \qquad (1)$$

where d is the distance of Io from the plasma equator and H is the plasma density scale height. The values of H were taken to be 1 R_J, 1.49 R_J, and 1.32 R_J for Io, Europa, and Ganymede, respectively, on the basis of equation (3) of *Hill and Michel* [1976] and plasma properties from *Kivelson et al.* [2004], e.g., temperatures and compositions from their Table 21.1. As seen for Io, Ganymede, and Europa, the correlations obtained for the Gaussian relation is similar to those for the linear correlations. In addition, prior observations by UVIS [*Steffl et al.*, 2004] showed temporal variations of torus densities as well as differences from the Voyager era [*Steffl et al.*, 2008]. However, our result shows the variations to be no more than 25%. This suggests the independence of Io's footprint brightness from the global properties of the plasma torus seen during the 10 year observation period.

[17] In Figure 3, the peak around 100° concurs with the estimate of the plasma equator near Ganymede (Figure 1). Although the current sheet is suggested to be nearly rigid [*Khurana and Schwarzl*, 2005], the plasma properties as well as the magnetic field configuration could change with local time and longitude (λ_{III}). Consequently, the variation of footprint brightness could be more time dependent, as seen in Figures 3 (top) and 3 (bottom). The trend in the Ganymede footprint brightness variation is not as clear as the trend in Io's. However, the same general trend is suggested, especially for the observation by the F115LP filter in 2007. At the same orbital longitude (λ_{III}) of Ganymede, different observing times gave different magnetic footprint brightnesses. As a result, Figure 6 shows a weaker correlation between Ganymede's distance from the plasma equator and its footprint brightness. As shown in Table 1, although the correlation coefficients for overall data are low, there is a difference among the results from individual filters of the ACS instrument. The correlation is low for the STIS observations, in which the brightness variation is comparable to the uncertainty. The best correlation is observed for the ACS F115LP filter (73.1%). This could be a result of different signal-to-noise ratios observed by different instruments (ACS and STIS). It should be noted that the variation of the brightness is comparable to the error bars considering Poisson uncertainty of

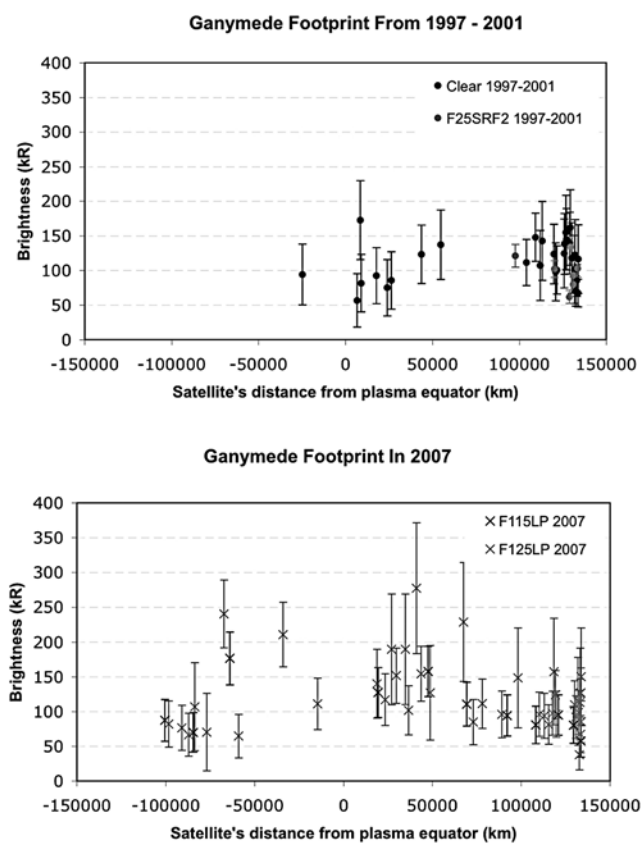

Figure 6. Same as Figure 5, but showing Ganymede's footprint brightness. The location of the plasma equator at Ganymede is assumed to be similar to the plasma equator at Io (Figure 1).

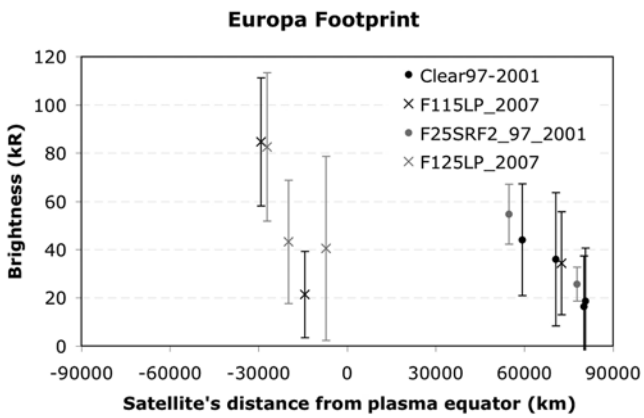

Figure 7. Same as Figure 5, but showing Europa's footprint brightness.

the background emission. If Ganymede's footprint brightness has a close connection with the local plasma density like Io's, this result could reflect the time variation of the current sheet density at Ganymede. According to *Schneider and Trauger* [1995], the dense plasma torus remains inside 7.5 R_J, while lower plasma densities extend to greater distances. Therefore, at Ganymede's orbital distance (15 R_J), which is considered to be the middle magnetosphere, the plasma system should be much different from the plasma system at Io's orbital distance (5.91 R_J). The differences include plasma density, structure, and solar wind influence. Since the plasma and magnetic field are tightly connected to each other, variations in the plasma density at Ganymede could cause the time variability of the footprint brightness. The difference in coefficients could be due to the variation of the footprint brightness related to Ganymede's interaction region, such as the variation of Jupiter's plasma equator location and density and energetic magnetospheric events, e.g., plasma ejections and reconnections in Ganymede's magnetosphere [*Grodent et al.*, 2009]. Furthermore, magnetic flux tubes at Ganymede's orbital distance (15 R_J) are very close to the magnetic field line connecting to the main oval (also seen in direct observations). While the emission of Ganymede's auroral footprint is expected to be equatorward of the main oval, at times, the footprints were seen to be very close or even blend into the main oval. Jupiter's main oval originates from the corotation breakdown region in the magnetosphere, near the interaction region at Ganymede. Jupiter's magnetic field simulated by the VIP4 model is carefully generated up to high-order spherical harmonic expansion including an empirical model for average conditions of the magnetodisc, while the effects of the solar wind are not included [*Connerney et al.*, 1998]. At Ganymede's orbit, the external influences become significant. Occasionally, Ganymede's footprint locations were not found exactly at the predicted locations. Previous observations [*Grodent et al.*, 2008a] compared the predicted and the observed Ganymede's footprint locations and found that the predictions are less accurate than the predictions of the locations of Io's footprints, especially in the region of the magnetic anomaly in the northern hemisphere.

[18] For Europa (Figure 4), the scattered footprint variation and low number of observed "good spots" cannot give us a clear indication of the connection between the footprint brightness and Europa's locations. In addition, Europa's magnetic footprints appear less bright than Io's and Ganymede's, suggesting that, within the limit of the low signal-to-noise ratio, the field-aligned currents related to the electrodynamic interaction at Europa are weaker than those at Io and Ganymede. The relation between Europa's footprint brightness and its distance from the plasma equator (using the same assumption in Ganymede's case) is shown in Figure 7. The correlation coefficient (Table 1) between Europa's distance from the plasma equator and the satellite's footprint brightness is low (46.1%). This may be a result of poor statistics and low signal-to-noise ratio. There is not enough certainty to draw conclusions about Europa's case.

6. Conclusion

[19] These results present the strong connection between Io's magnetic footprint brightness and the density of the plasma torus in which Io is embedded. While the strength of the interaction between Io and Jupiter's magnetosphere is determined by the ratio of the effective conductivity of Io (including Pedersen, Hall, and pickup conductivities) to the Alfvén conductivity [*Hill et al.*, 1983], the variation of plasma density near the satellite is more directly related to the conductivity due to the mass pickup. Moreover, the Alfvén conductivity is determined by the magnetic field and current loop that close far from Io. Our results present the strong connection between Io's magnetic footprint brightness and the density of the plasma torus in which Io is embedded. Therefore, the pickup process is an important controlling factor of Io's footprint brightness. During 10 years of HST observations, the variation of Io's magnetic footprint as a function of Io's location has not changed much, suggesting that it is time independent. Observations of Ganymede's and Europa's magnetic footprints, which appear to be time variable but with a low signal-to-noise ratio, are also presented. These interactions may reflect the stronger influence of the current sheet at greater distances from Jupiter. Farther away from Jupiter than Io, Ganymede and Europa are located in regions where the plasma density is lower and the possibility of solar wind influence is higher.

[20] Modeling the structure of Jupiter's plasma density in the torus and current sheet will be a powerful tool to describe the variation of the footprint brightness in detail. Along with magnetic field modeling, this future work will be another stepping stone to understanding more about Jupiter's magnetosphere and the unique electrodynamic interactions with Jovian satellites.

[21] **Acknowledgments.** We acknowledge constructive discussions with William Smyth, Nick Schneider, and Fran Bagenal. This work is based on observations with the NASA/ESA Hubble Space Telescope, obtained at the Space Telescope Science Institute, which is operated by the AURA Inc. for NASA. This research was supported by NASA grant HST-GO-10862.01-A from the Space Telescope Science Institute to Boston University. J.D.N. was supported throughout the course of this study by STFC grant PP/E000983/1.

[22] Wolfgang Baumjohann thanks Sébastien Hess and another reviewer for their assistance in evaluating this paper.

References

Bagenal, F. (1994), Empirical model of the Io plasma torus: Voyager measurement, *J. Geophys. Res.*, *99*, 11,043–11,062, doi:10.1029/93JA02908.

Bagenal, F., and J. D. Sullivan (1981), Direct plasma measurements in the Io torus and inner magnetosphere of Jupiter, *J. Geophys. Res.*, *86*, 8447–8466, doi:10.1029/JA086iA10p08447.

Bigg, E. L. (1964), Influence of the satellite Io on Jupiter's decametric radiation, *Nature*, *203*, 1008–1009, doi:10.1038/2031008a0.

Bonfond, B., J.-C. Gérard, D. Grodent, and J. Saur (2007), Ultraviolet Io footprint short timescale dynamics, *Geophys. Res. Lett.*, *34*, L06201, doi:10.1029/2006GL028765.

Bonfond, B., D. Grodent, J.-C. Gérard, A. Radioti, J. Saur, and S. Jacobsen (2008), UV Io footprint leading spot: A key feature for understanding the UV Io footprint multiplicity?, *Geophys. Res. Lett.*, *35*, L05107, doi:10.1029/2007GL032418.

Broadfoot, A. L., et al. (1979), Extreme ultraviolet observations from Voyager 1 encounter with Jupiter, *Science*, *204*, 979–982, doi:10.1126/science.204.4396.979.

Carlson, H. C., Jr., and A. Egeland (1995), The aurora and the auroral ionosphere, in *Introduction to Space Physics*, edited by M. G. Kivelson and C. T. Russell, pp. 459–498, Cambridge Univ. Press, Cambridge, U. K.

Clarke, J. T., L. Ben Jaffel, and J.-C. Gérard (1998), Hubble Space Telescope imaging of Jupiter's UV aurora during the Galileo orbiter mission, *J. Geophys. Res.*, *103*, 20,217–20,236, doi:10.1029/98JE01130.

Clarke, J. T., D. Grodent, S. W. H. Cowley, E. J. Bunce, P. Zarka, J. E. P. Connerney, and T. Satoh (2004), Jupiter's aurora, in *Jupiter: The Planet, Satellites and Magnetosphere*, edited by F. Bagenal, T. E. Dowling, and W. B. Mckinnon, pp. 639–670, Cambridge Univ. Press, Cambridge, U. K.

Clarke, J. T., et al. (2009), Response of Jupiter's and Saturn's auroral activity to the solar wind, *J. Geophys. Res.*, *114*, A05210, doi:10.1029/2008JA013694.

Connerney, J. E. P., R. Baron, T. Satoh, and T. Owen (1993), Images of excited H_3^+ at the foot of the Io flux tube in Jupiter's atmosphere, *Science*, *262*, 1035–1038, doi:10.1126/science.262.5136.1035.

Connerney, J. E. P., M. H. Acuña, N. F. Ness, and T. Satoh (1998), New models of Jupiter's magnetic field constrained by the Io flux tube footprint, *J. Geophys. Res.*, *103*, 11,929–11,939, doi:10.1029/97JA03726.

Cowley, S. W. H. (1998), The earth's magnetosphere, in *From the Sun: Auroras, Magnetic Storms, Solar Flares, Cosmic Rays*, edited by S. T. Suess and B. T. Tsurutani, 13 pp., AGU, Washington, D. C.

Crary, F. J. (1997), On the generation of an electron beam by Io, *J. Geophys. Res.*, *102*(A1), 37–49, doi:10.1029/96JA02409.

Crary, F. J., and F. Bagenal (1997), Coupling the plasma interaction at Io to Jupiter, *Geophys. Res. Lett.*, *24*, 2135–2138.

Delamere, P. A., F. Bagenal, R. Ergun, and Y.-J. Su (2003), Momentum transfer between the Io plasma wake and Jupiter's ionosphere, *J. Geophys. Res.*, *108*(A6), 1241, doi:10.1029/2002JA009530.

Gérard, J.-C., J. Gustin, D. Grodent, P. Delamere, and J. T. Clarke (2002), Excitation of the FUV Io tail on Jupiter: Characterization of the electron precipitation, *J. Geophys. Res.*, *107*(A11), 1394, doi:10.1029/2002JA009410.

Gérard, J. C., A. Saglam, D. Grodent, and J. T. Clarke (2006), Morphology of the ultraviolet Io footprint emission and its control by Io's location, *J. Geophys. Res.*, *111*, A04202, doi:10.1029/2005JA011327.

Goertz, C. K. (1980), Io's interaction with the plasma torus, *J. Geophys. Res.*, *85*, 2949–2956, doi:10.1029/JA085iA06p02949.

Goldreich, P., and D. Lynden-Bell (1969), Io, a Jovian unipolar inductor, *Astrophys. J.*, *156*, 59–78, doi:10.1086/149947.

Grodent, D., J. T. Clarke, J. Kim, J. H. Waite Jr., and S. W. H. Cowley (2003), Jupiter's main auroral oval observed with HST STIS, *J. Geophys. Res.*, *108*(A11), 1389, doi:10.1029/2003JA009921.

Grodent, D., B. Bonfond, J.-C. Gérard, A. Radioti, J. Gustin, J. T. Clarke, J. Nichols, and J. E. P. Connerney (2008a), Auroral evidence of a localized magnetic anomaly in Jupiter's northern hemisphere, *J. Geophys. Res.*, *113*, A09201, doi:10.1029/2008JA013185.

Grodent, D., J.-C. Gérard, A. Radioti, B. Bonfond, and A. Saglam (2008b), Jupiter's changing auroral location, *J. Geophys. Res.*, *113*, A01206, doi:10.1029/2007JA012601.

Grodent, D., B. Bonfond, A. Radioti, J.-C. Gérard, X. Jia, J. D. Nichols, and J. T. Clarke (2009), Auroral footprint of Ganymede, *J. Geophys. Res.*, *114*, A07212, doi:10.1029/2009JA014289.

Gurnett, D. A., and C. K. Goertz (1981), Multiple Alfven wave reflections excited by Io: Origin of the Jovian decametric arcs, *J. Geophys. Res.*, *86*(A2), 717–722, doi:10.1029/JA086iA02p00717.

Hess, S., B. Cecconi, and P. Zarka (2008), Modeling of Io-Jupiter decameter arcs, emission beaming and energy source, *Geophys. Res. Lett.*, *35*, L13107, doi:10.1029/2008GL033656.

Hill, T. W. (2004), Auroral structures at Jupiter and Earth, *Adv. Space Res.*, *33*, 2021–2031, doi:10.1016/j.asr.2003.05.037.

Hill, T. W., and F. C. Michel (1976), Heavy ions from the Galilean satellites and the centrifugal distortion of the Jovian magnetosphere, *J. Geophys. Res.*, *81*, 4561–4565, doi:10.1029/JA081i025p04561.

Hill, T. W., A. J. Dessler, and C. K. Goertz (1983), Magnetospheric models, in *Physics of the Jovian Magnetosphere*, edited by A. J. Dessler, pp. 353–394, Cambridge Univ. Press, New York.

Jacobsen, S., F. M. Neubauer, J. Saur, and N. Schilling (2007), Io's nonlinear MHD wave field in the heterogeneous Jovian magnetosphere, *Geophys. Res. Lett.*, *34*, L10202, doi:10.1029/2006GL029187.

Khurana, K. K., and H. K. Schwarzl (2005), Global structure of Jupiter's magnetospheric current sheet, *J. Geophys. Res.*, *110*, A07227, doi:10.1029/2004JA010757.

Kivelson, M. G. (2005), The current systems of the Jovian magnetosphere and ionosphere and predictions for Saturn, *Space Sci. Rev.*, *116*, 299–318, doi:10.1007/s11214-005-1959-x.

Kivelson, M. G., F. Bagenal, W. S. Kurth, F. M. Neubauer, C. Paranicas, and J. Saur (2004), Magnetospheric interactions with satellites, in *Jupiter: The Planet, Satellites and Magnetosphere*, edited by F. Bagenal, T. E. Dowling, and W. B. Mckinnon, pp. 513–536, Cambridge Univ. Press, Cambridge, U. K.

McPherron, R. L. (1995), Magnetospheric dynamics, in *Introduction to Space Physics*, edited by M. G. Kivelson and C. T. Russell, pp. 420–423, Cambridge Univ. Press, Cambridge, U. K.

Moncuquet, M., F. Bagenal, and N. Meyer-Vernet (2002), Latitudinal structure of outer Io plasma torus, *J. Geophys. Res.*, *107*(A9), 1260, doi:10.1029/2001JA900124.

Neubauer, F. M. (1980), Nonlinear standing Alfvén wave current system at Io: Theory, *J. Geophys. Res.*, *85*, 1171–1178, doi:10.1029/JA085iA03p01171.

Nichols, J. D., J. T. Clarke, J.-C. Gérard, D. Grodent, and K. C. Hansen (2009), The variation of different components of Jupiter's auroral emission, *J. Geophys. Res.*, *114*, A06210, doi:10.1029/2009JA014051.

Nichols, J. D., J. T. Clarke, S. W. H. Cowley, J. Duval, A. J. Farmer, J.-C. Gérard, D. Grodent, and S. Wannawichian (2008), Oscillation of Saturn's southern auroral oval, *J. Geophys. Res.*, *113*, A11205, doi:10.1029/2008JA013444.

Saur, J., F. M. Neubauer, J. E. P. Connerney, P. Zarka, and M. G. Kivelson (2004), Plasma interaction of Io with its plasma torus, in *Jupiter: The Planet, Satellites and Magnetosphere*, edited by F. Bagenal, T. E. Dowling, and W. B. Mckinnon, pp. 537–560, Cambridge Univ. Press, Cambridge, U. K.

Schneider, N. M., and J. T. Trauger (1995), The structure of the Io torus, *Astrophys. J.*, *450*, 450–462, doi:10.1086/176155.

Serio, A. W., and J. T. Clarke (2008), The variation of Io's auroral footprint brightness with the location of Io in the plasma torus, *Icarus*, *197*, 368–374, doi:10.1016/j.icarus.2008.03.026.

Stallard, T. S., et al. (2008), Jovian-like aurorae on Saturn, *Nature*, *453*, 1083–1085, doi:10.1038/nature07077.

Steffl, A. J., I. Stewart, and F. Bagenal (2004), Cassini UVIS observations of the Io plasma torus. I. Initial results, *Icarus*, *172*, 78–90, doi:10.1016/j.icarus.2003.12.027.

Steffl, A. J., P. A. Delamere, and F. Bagenal (2008), Cassini UVIS observations of the Io plasma torus. IV. Modeling temporal and azimuthal variability, *Icarus*, *194*, 153–165, doi:10.1016/j.icarus.2007.09.019.

Vincent, M. B., et al. (2000), Jupiter's polar regions in the ultraviolet as imaged by HST/WFPC2: Auroral-aligned features and zonal motions, *Icarus*, *143*, 205–222, doi:10.1006/icar.1999.6233.

Wannawichian, S., J. T. Clarke, and D. H. Pontius (2008), Interaction evidence between Enceladus' atmosphere and Saturn's magnetosphere, *J. Geophys. Res.*, *113*, A07217, doi:10.1029/2007JA012899.

J. T. Clarke and S. Wannawichian, Center for Space Physics, Boston University, 725 Commonwealth Ave., Boston, MA 02215, USA. (suwichaw@bu.edu)

J. D. Nichols, Department of Physics and Astronomy, University of Leicester, Leicester LE1 7RH, UK.